The Ultraviolet Spectrum of HH 24A and its Relation to Optical Spectra

K.H. Böhm[1] and A. Noriega-Crespo

Astronomy Department, FM-20, University of Washington

Seattle, WA 98195.

J. Solf[1]

Max-Planck-Institut für Astronomie

Kömnigstuhl 17, 6900 Heidelberg, Germany

and

E.W. Brugel[1]

Center for Astrophysics and Space Astronomy

University of Colorado, Boulder, CO 80309

[1] Guest Observer with the *International Ultraviolet Explorer* which is sponsored and operated jointly by the National Aeronautics and Space Administration, the European Space Agency, and the Science Research Council of the United Kingdom.

Abstract

We have studied the spectrum of the brightest part (HH 24A) of the complex Herbig-Haro object HH 24 in the short wavelength (1300 Å $\lesssim \lambda \lesssim$ 1930) ultraviolet range. The object is of special interest since it is known that in the optical range the continuum is due to dust scattered light originating in a young stellar object while the shock excited emission lines are formed in HH 24A itself.

The ultraviolet spectrum is definitely detected in three observations with exposure times of 560 to 680 min. It is, however, sufficiently faint that corrections for the IUE "artifact spectrum" (as described by Crenshaw *et al.*) have to be applied. The spectrum shows only a continuum or a quasi-continuum and is not comparable not to that of the typical high excitation object like HH1 or HH2 nor to that of a low excitation object like HH 43 or HH 47. The HH 24A spectrum does not resemble the spectra of the T Tauri stars observed with IUE. It is therefore not probable that, as in the optical range, we are seeing dust scattered light from a T Tauri or similar star.

Two of the three spectra show a surprisingly similar detailed wavelength structure. If we assume that this means that these structures are real then no convincing explanation of the spectrum seems yet to be available. If, on the other hand, we are satisfied with a crude interpretation of the average wavelength dependence (ignoring detailed structures of the spectrum) the interpretation as a collisionally enhanced two-photon continuum may be acceptable.

A study of the spatial distribution of the ultraviolet continuum emission shows that this distribution is considerable wider than that of the optical forbidden line emission, *e.g.*, in the [S II] 6716/6731 lines.

1. Introduction

Herbig-Haro (HH) objects are shock-excited regions in the environment of recently formed stars. They are in many cases (but not always) connected with the "working surfaces" or with internal shocks of bipolar jets from young stars (see *e.g.*, Mundt 1987; Reipurth 1991; Edwards, Ray & Mundt 1991). A number of HH objects have been observed with IUE (see *e.g.*, Ortolani & d'Odorico 1980; Böhm, Böhm-Vitense & Brugel 1981; Schwartz 1983a,b; Brugel, Shull & Seab 1982; Böhm & Böhm-Vitense 1984; Cameron & Liseau 1990). Recent review articles about the ultraviolet emission of HH objects have been published by Brugel (1989) & Böhm (1990).

The fact that HH objects can be observed with IUE is somewhat surprising because they are relatively faint in the optical ($m_v \sim 16$ or fainter) and they do show moderate reddening (*e.g.*, E(B-V) $\sim$ .43 in the case of HH 1, see *e.g.*, Brugel, Böhm & Mannery 1981). For a number of years (until the work by Cameron & Liseau 1990 became available) only 5 HH objects had been detected with IUE, namely HH1 (Ortolani & d'Odorico 1980; Böhm *et al.* 1981), HH 2 (Böhm-Vitense *et al.* 1982; Brugel *et al.* 1982), HH 32 (Böhm & Böhm-Vitense 1984), HH 43 and HH 47 (Schwartz 1983 a, b). Of these five objects, three (HH 1, HH 2 and HH 32) are high excitation and two HH 43 and HH 47 are low excitation objects. It turns out that these two groups differ much more drastically in their UV (IUE) spectra than in their their optical spectra (although differences in their optical spectra are by no means negligible, see *e.g.*, Böhm, Brugel & Mannery 1980). In the UV the three high excitation objects show C IV 1550 and C III] 1909 which are by far the strongest emission lines, while the two low excitation spectra are dominated by fluorescent H_2 emission lines with very few (if any) ionic lines. It has been surprising that the observed IUE spectra of HH objects form such two completely disconnected groups and that no intermediate spectra are seen. This may or may not be due to the very small sample of HH objects observed so far with IUE.

For this reason it is very important to try to obtain IUE spectra of additional Herbig-Haro objects. It is to be expected that these spectra will be faint. But the problem is

important enough to make the attempt worth while.

Considerable progress has been made recently in this field by Cameron & Liseau (1990). They have been able to carry out IUE observations of the HH objects HH 7, HH 11 and HH 29 which all had not been observed before with IUE. Among these HH 7 and HH 11 are well known low excitation objects (see *e.g.*, Böhm, Brugel & Olmsted 1983; Goodrich 1986; Solf & Böhm 1987). HH 7 is very faint and it is really impressive that Cameron and Liseau (1990) have been able to detect its UV emission. They did this by developing new reduction procedures and an especially sophisticated background subtraction method. The ultraviolet SWP spectrum of HH 7 (and HH 11) shows only a continuum. According to Cameron & Liseau (1990) the absence of fluorescent H_2 lines is compatible with the observed intensity of the near infrared H_2 lines and the extinction of this object. The continuum is bluer than in any other HH object. Since HH7 shows lower excitation than any other HH object (see, *e.g.*, Solf & Böhm 1987; Böhm & Solf 1990) it is clear that the results do not fit into the sequence of SWP spectra of high and low excitation objects as defined by HH 1, HH 2, HH 32, HH 43 and HH 47 (see above). HH 7 does not show the SWP continuous energy distribution seen in both the high and the low excitation objects. This indicates that the UV emission of HH objects (in the SWP range) does not follow the simple rules which were indicated by the studies of only HH 1, HH 2, HH 32, HH 43 and HH 47 and that ultraviolet studies of additional HH objects are needed.

For a number of reasons HH 24A is an interesting candidate for an IUE study. Although very faint in the ultraviolet, it has been detected already in the SWP and LWP ranges (Lee *et al.* 1988; Brugel 1989). It is an object which is of special interest for at least two reasons. It shows moderate excitation (Brugel *et al.* 1981) and lies in this sense between the well studied really high excitation objects HH 1, HH 2, HH 32 and the low excitation objects HH 43 and HH 47. It also has the peculiar property that its optical continuum shows surprisingly large linear polarization (~25%) (Strom, Strom & Kinman 1974; Schmidt & Miller 1979) indicating that it is due to dust scattered light which probably originally comes

from the young stellar object identified by Strom *et al.* (1974) as the "source" of HH24.

The Herbig-Haro object 24 is fairly extended and quite complex (Herbig 1974; Solf 1987). The present ultraviolet observations are restricted to the brightest condensation HH 24A and its immediate environment (see Figure 1).

Using IUE observations we hope to answer the following questions:

1. Since the excitation shown by the optical spectrum of HH24 is intermediate between that of high and low excitation objects, does HH 24 possibly show a SWP spectrum intermediate between the vastly different spectra of high excitation and low excitation objects?

2. Is the continuum in the SWP range (like the optical continuum) due to dust scattered light which originally comes from the young stellar object which forms the "source" of HH 24?

It is clear that it is not easy to answer these questions because HH 24 (like HH 7 and HH 11) is very faint in the SWP range of IUE.

2. Observations and Reductions

We have obtained two SWP low resolution spectra of HH 24A (SWP 38033 and 38102) using in both cases two-shift exposures (ESA – US1) in January 1990. Some basic information about these observations is listed in Table 1. Both observations were taken with the large aperture using low resolution. It is important to note that the "aperture orientation angle" (*i.e.*, the position angle of the aperture) differed only slightly for these two observations (307° to 320°). This means that as a reasonable approximation we can take an average of both spectra for the determination of the spatial distribution of the ultraviolet emission. Moreover, the average position angle (314°) of the aperture for the two observations agrees (accidentally) well with the orientation of the elongated HH 24A (see Figure 1). In this sense the observations are optimal for the determination of a spatially resolved spectrum of HH 24A. We have determined both the spatially resolved ("line-by-line") and integrated

spectra from these two observations, SWP 38033 and 38102 using standard reduction procedures (see *e.g.*, Turnrose & Thomson 1984).

For the determination of the merged spectrum we have also used an earlier observation (SWP 21518) by Brugel & Shull with a 560 minute exposure time (see Table 1).

In order to obtain useful information about the energy (*i.e.*, wavelength) distribution of the ultraviolet spectrum of this object we have to take into account the following. The intensities are moderately but not very much larger than the "artifact spectrum" (Crenshaw, Bruegman & Norman 1990) which is seen in long exposures of the blank sky. We have therefore subtracted the "reference artifact spectrum" for long exposures (see Crenshaw *et al.* 1990, Figure 7) from the measured flux spectrum. Examples of this can be seen in Figures 3 and 4 (see below) where we show the average of the short wavelength IUE spectra, the IUE artifact spectrum and the difference between the observed spectrum and the artifact spectrum. The fact that this difference is positive almost everywhere gives us some confidence that the procedure is at least qualitatively correct.

We have also calculated the de-reddened (merged) spectrum. The reddening of HH 24A is, however, not well known. Brugel *et al.* (1981) estimated that E(B-V) $\sim$ 0.71 using the observed Balmer decrement. We consider this now as an overestimate. In the attempt to reproduce the Balmer decrement we had put too much weight on the lines Hγ and Hδ for which the spectrophotometric data were not yet as good as we had hoped. Using only Hα and Hβ one finds a value of E(B-V) in the range between 0.4 and 0.5. Unfortunately the infrared [S II] lines have not yet been detected in HH 21A. Therefore Miller's (1968) method which has been successfully applied in brighter objects (see *e.g.*, Böhm, Siegmund & Schwartz 1976; Brugel *et al.* 1981; Solf, Böhm & Raga 1988) cannot yet be used for HH 24A.

For our reductions we have now adopted an E(B-V) = 0.15. We have dereddened the data for both the R=3.1 and the R=5.4 curves from Cardelli, Clayton & Mathis (1988). These two extinction curves correspond approximately to the earlier "Seaton" (1979) and the "θ

Orionis" curve (Bohlin & Savage 1981). It is not yet entirely clear which type of extinction curve is the most appropriate for most HH objects. Circumstantial evidence seemed to favor a θ Orionis curve (see *e.g.*, Böhm & Böhm-Vitense 1984; Schwartz, Dopita & Cohen 1985). Recently, however, Böhm, Raga & Binette (1990) have compared relative line fluxes of strong UV and optical lines in HH1 and HH2 to predictions for bow shock models and have concluded that, surprisingly, the "Seaton" curve (curve with R=3.1 of Cardelli *et al.* 1988) leads to better agreement between observed line fluxes and predictions of bow shock models than the θ Orionis curve (curve with R=5.4 of Cardelli *et al.* 1988). Since this conclusion does not agree with the earlier ones based on more intuitive arguments we shall for the moment consider the question as undecided and we shall therefore present reddening corrected energy distributions for both the R=31 (Seaton) and R=5.4 ("θ Orionis") curves.

For the determination of the spatial variation of the continuum emission we have studied the line-by-line spectra, binning two "lines" into a single spectrum. Because of the low signal-to-noise ratio we shall only consider the spatial variation of the total emission in the broad wavelength interval 1600 Å $\lesssim \lambda \lesssim$ 1800 Å. Studying this interval has the advantage that the SWP camera is more sensitive in this region than at shorter wavelengths. The resulting spatial distribution has been corrected for the (somewhat) varying sensitivity along the main axis of the large aperture (see Clarke & Moos 1981). We also compare the UV emission distribution to that of the (optical) emission in the [S II] 6716/6731 lines. For this purpose we use a narrow band image of HH 24 in the light of the [S II] lines kindly provided by R. Mundt which was obtained on the 3.5-m telescope of the Calar Alto Observatory. The optical data are extracted from the CCD image in a way analogous to the one described by Lee *et al.* (1988). We select an area on the CCD image corresponding to the size (23" × 11") and orientation of the projected slit aperture used with the IUE. The (one-dimensional) distribution of the [S II] intensity along the direction of the slit aperture is obtained by integration of the detected line emission along the short axis of the selected area on the CCD image. The result then has to be convolved with the IUE point-spread function (as

given by de Boer & Meade 1981) to make it comparable to the IUE results. Ideally it would be more appropriate to leave the optical data as they are and to de-convolve the IUE data but attempts to do this have not been successful (see Lee *et al.* 1988).

3. Results and Discussion

3.1. Merged Spectra

We have studied three spectra, namely SWP 38033, SWP 38102 (both taken in January 1990) and SWP 21518 (taken in 1983, see also Table 1). The spectra SWP 38102 (taken 1990) and SWP 21518 (taken 1983) agree surprisingly well. This is illustrated in Figure 2 which compares the flux distributions in SWP 38102 to the distribution which we get after averaging over SWP 38102 and SWP 21518. These show the directly observed spectra uncorrected for reddening and for the effects of the "artifact spectrum" (see Crenshaw *et al.* 1990). Surprisingly the spectrum SWP 38033 differs more strongly from SWP 38102 than SWP 21518 although SWP 38033 and SWP 38102 were taken only two weeks apart. It is hard to believe that the good agreement between SWP 38102 and SWP 21518 could be purely accidental. On the other hand, we do not see any obvious reason why SWP 39033 should be ignored. In the following we shall therefore use averages over the three spectra SWP 38033, SWP 38102 and SWP 21518. Only in Figure 4 we show for comparison purposes the spectrum (uncorrected for reddening) which we would obtain if we would ignore SWP 39033.

In Figure 3 and Figure 4 we show for both cases the average observed spectrum, the artifact spectrum and the difference between these two which we identify tentatively with the real observed spectrum (uncorrected for reddening). The figures show a few interesting facts. 1. There is no indication of identifiable emission lines. (Whether this is due to the low signal to noise ratio or whether the spectrum is really continuous or quasi-continuous is not yet clear.) 2. All regions where the flux values are very low are also characterized by very uncertain flux values because they are obtained by the subtraction of two almost equal but rather uncertain fluxes (of the HH 24 and the artifact spectrum). 3. The spectra do not

show the pronounced maximum near 1580 Å which the typical high excitation objects HH 1 and HH 2 (Böhm *et al.* 1987) and the typical low excitation objects HH 43 and HH 47 (Böhm, Scott & Solf 1991) exhibit and which has been tentatively interpreted by a fluorescent H_2 continuum.

In Figure 5 we show the reddening corrected energy distributions (see also chapter 2) for the two different average energy distributions that we have discussed above. We present data corrected with the Seaton curve as well as results corrected with the θ Orionis curve. If we take the results at face value it is not easily possible to explain the energy distribution. In principle, one might consider one of the two following types of explanations: a. Since we know that the optical continuum in HH 24A is very probably due to dust scattering of the continuum from a young stellar object (Strom *et al.* 1974; Schmidt & Miller 1979) it would be plausible to assume that the ultraviolet continuum is also due to dust scattering. b. It is, of course, also possible that we see a continuum or a quasi-continuum formed in the HH object itself (the continuum may be influenced by emission lines which are not individually detected because of the low signal-to-noise ratio). It is believed that in the brighter HH objects the continuum is due to a collisionally enhanced two-photon continuum (Brugel *et al.* 1982; Dopita, Binette & Schwartz 1982) which in HH 1, HH 2, HH 43 and HH 47 seems to be modified by the addition of a fluorescent H_2 continuum.

In view of the faintness of the spectrum the question arises whether the structures which are seen (as a function of wavelength) are real. Although they are very hard to explain and we might be inclined to dismiss them as not real, there remains the surprising agreement between SWP 38102 and SWP 21518 (see Figure 2). It may, of course, be that the artifact spectrum is sufficiently uncertain so that in the difference (observed spectrum – artifact spectrum) we obtain structures which are not real. If we accept one of the spectra presented in Figure 5 as correct or even as very approximately correct then we have to conclude that we are not seeing a dust scattered spectrum from an active or moderately active T Tauri star like *e.g.*, RW Aurigae or GW Orionis (see *e.g.*, Imhoff & Appenzeller 1987). Both the overall

distribution as well as the individual spectral features look quite different in HH 24. Could the observed continuum be due to collisionally enhanced two photon emission like *e.g.*, in HH 1? This may be marginally possible if we assume that all the individual spectral features are not real. In a very approximate way the energy distribution has an overall λ-dependence which shows some vague similarity to the two photon emission coefficient. This is shown in Figure 6 where we compare the (arbitrarily scaled) two photon continuum of hydrogen to the observational results which have been corrected for reddening using the Seaton curve. The observational data have been "smoothed" (using a running mean over 60 Å intervals). Even so the observed energy distribution shows still a lot of structure. We are definitely not claiming that Figure 6 proves that the continuum in HH 24 must be explained as a two photon continuum.

As shown in Figure 2 there is a good chance that the apparent wavelength structure of the observed continuum is real. In this case an explanation in terms of two photon emission is not possible. On the other hand the assumption that we see the dust scattered spectrum of a T Tauri star leads to even worse discrepancies.

The situation is somewhat similar to that of the other two faint HH objects, HH 7 and HH 11 (Cameron & Liseau 1990) for which faint ultraviolet spectra have also been detected but for which the energy distributions are also difficult to interpret. (They are, however, very different from that of HH 24.)

3.2. The Spatial Distribution of Ultraviolet Emission and Comparison to Optical Data

In view of the difficulties in deriving the merged spectra of HH 24 it might seem surprising that we can even consider to measure the spatial distribution of the ultraviolet emission. This is, however, possible because we are binning the data in large wavelength intervals. We found that we can obtain the relatively best data if we consider the spatial variation of the intensity integrated over the wavelength interval from 1600 to 1800 Å. The interval contains a sufficient number of pixels (see also chapter 2). Moreover, the SWP camera is considerably

more sensitive in this wavelength range than at shorter wavelengths (see chapter 2).

We have measured the line-by-line spectra for both SWP 38033 and SWP 38102 and find very similar spatial distributions (Figure 7). In the following we shall therefore restrict the discussion to the average spatial distribution derived from both spectra (Figure 8).

The spatial distributions have been corrected for the (somewhat) varying sensitivity along the main axis of the large aperture (Clarke & Moos 1981). For comparison purposes we also show the point spread function for the IUE SWP camera at $\lambda \sim 1600$ Å and the one dimensional distribution of the [S II] 6716, 6731 lines in the optical range (Figure 8). In order to make the optical data comparable to the ultraviolet data the spatial distribution of the [S II] 6716, 6731 emission has been convolved with the IUE point spread function (see chapter 2). Figure 8 shows that the ultraviolet emission distribution (for $1600 \lesssim \lambda \lesssim 1800$ Å) has a halfwidth which is about a factor 2 larger than that of the spatial distribution of the [S II] line emission. This is compatible with somewhat similar results found by Lee *et al.* (1988) for a number of HH objects.

The UV emission in the HH 24A distribution looks rather asymmetric with an extended "wing" towards the SE (which is the left hand side of Figure 8). This may be related to the extended emission visible in Figure 1 (using a wavelength range 6200 Å $\lesssim \lambda \lesssim$ 7000 Å) in this region. In the region of this wing there lies also a very small hump in the [S II] emission which is clearly visible in the original (not convolved) [S II] emission distribution.

All this may be an indication that the short wavelength UV spectrum of HH 24A contains contributions from both intrinsic emission (*e.g.*, due to a two photon continuum) and dust scattered light. As discussed above the observed wavelength dependence of the merged spectrum does not seem to be compatible with the dust scattering of light from a young star, especially a T Tauri star. The wavelength distribution did, however, show some crude similarity to a two photon continuum although in detail there were considerable differences. The merged spectrum could be a "mixture" of a two photon continuum and of a dust

scattered continuum of a young stellar object. Possibly the extended SE wing of the emission distribution in Figure 8 is perhaps mostly due to dust scattering. This would make it understandable that this wing is also visible in Figure 1, an image taken in a broad band wavelength band (6200-7000 Å) with an important continuum contribution.

It remains unclear why the ultraviolet spectrum of HH 24A does not show emission lines. In a typical high excitation HH object like HH 2 the C IV 1550 and the C III] 1909 line peaks are roughly five times higher than the underlying continuum (in the low resolution mode). We would expect that even in a very noisy spectrum like that of HH 24A such strong lines would be visible. On the other hand, HH 24A does not show as high an excitation as HH 2. This is indicated by the observed [O III] 5007/Hβ ratio which is $\sim$0.68 in HH 2H but only 0.26 in HH 24A (Brugel *et al.* 1981). Present shock models are not yet accurate enough to state convincingly whether the corresponding decrease in "excitation" (*i.e.*, in shock velocity) would really make a line like C III] 1909 undetectable in HH 24A. A final clarification will probably be only possible if spectra with considerably better signal-to-noise ratios than the present IUE spectra can be obtained.

4. Conclusions

The short wavelength (SWP) IUE spectrum of HH 24A has been studied using three long exposure (560 min – 680 min) observations. The spectrum is well-detected in the range 1300 Å$\lesssim \lambda \lesssim$ 1900 Å although the intensities are only moderately larger than those for the "IUE artifact spectrum" (Crenshaw *et al.* 1990). Two of the three spectra agree surprisingly well even in some details of the spectral energy distribution. The spectra have been corrected for the presence of the artifact spectrum. We have studied both the merged spectra and the line-by-line spectra. From the latter ones we have determined the spatial distribution of the ultraviolet emission. Because of the low signal-to-noise ratio relatively drastic wavelength binning was required (we have used a 200 Å interval).

The merged spectrum shows only a continuum or quasi-continuum (unresolved emission

lines?). No individual emission lines have been detected. The detailed observed wavelength structure is not understood. We find that it cannot be explained as the dust scattered ultraviolet spectrum of a T Tauri star although the optical spectrum of HH 24A (which is highly polarized, see Strom *et al.* 1974; Schmidt & Miller 1979) is believed to show the dust scattered continuum of a T Tauri star. In a very crude approximation the continuum has some similarity to a two photon continuum provided we ignore some details in the spectral structure.

The spatial distribution (at a position angle of 313°) of the ultraviolet emission has been studied only for the integrated wavelength interval 1600 Å $\lesssim \lambda \lesssim$ 1800 Å. The core of the spatial distribution of the ultraviolet emission is about twice as wide as the one of the optical [S II] 6716/6731 lines. In addition, the ultraviolet distribution shows an extended wing towards the SE which covers slightly more than 6" (seconds of arc). This may be related to a qualitatively similar structure seen in an observation in the range 6200 Å $\lesssim \lambda \lesssim$ 7000 Å shown in Figure 1. We speculate that this wing may be due to dust scattered light and that the core of the distribution may be due to a superposition of a two photon continuum formed in situ and some contribution of dust scattered starlight.

We gratefully acknowledge the assistance of the IUE Observatory staff at the Goddard Space Flight Center and the Villafranca Observing Station. Some of the reductions have been carried out at the Regional Data Analysis Facility at the University of Colorado in Boulder which is operated under NASA contract NAS 5-28731. We are also grateful to Peter Garnavich for his help with the RDAF software. We also thank Michael Crenshaw for providing use with the files of his "reference artifact spectrum." We are very grateful to Reinhard Mundt for making available a narrow-band CCD image of HH 24 in the light of the [S II] lines. K.H.B.'s and A.N.C.'S research has been supported by NASA grant NAG 5-45 and NSF grant AST 89 18458.

References

Bohlin, R. C. & Savage, B. D. 1981, ApJ, 249, 109

Böhm, K. H. 1990, in Evolution in Astrophysicas, IUE Astronomy in the Era of New Space Missions, ESA Conf. Proc. SP-310, p. 23.

Böhm, K. H. & Böhm-Vitense, E. 1984, ApJ, 277, 216

Böhm, K. H., Böhm-Vitense, E. & Brugel, E. 1981, ApJ, 245, L113

Böhm, K. H., Brugel, E. W. & Mannery, E. 1980, ApJ, 235, L137

Böhm, K. H., Brugel, E. W. & Olmsted, E. 1983, A& A, 125, 23

Böhm, K. H., Bührke, T., Raga, A. C., Brugel, E. W., Witt, A. N. & Mundt, R. 1987, ApJ, 316, 349

Böhm, K. H., Raga, A. C. & Binette, L. 1991, PASP, 103, 85

Böhm, K. H., Scott, D. M. & Solf, J. 1991, ApJ, 371, 218

Böhm, K. H., Siegmund, W. A. & Schwartz, R. D. 1976, ApJ, 203, 399

Böhm, K. H. & Solf, J. 1990, ApJ, 348, 297

Böhm-Vitense, E., Böhm, K. H., Cardelli, J. A. & Nemec, J. M. 1982, ApJ, 262, 224

Brugel, E. W. 1989, in Low Mass Star Formation and Pre-Main Sequence Objects, ed. B. Reipurth, ESO Conf. and Workshop Proceedings, No. 33, p. 311

Brugel, E. W., Böhm, K. H. & Mannery, E. 1981, ApJS, 47, 117

Brugel, E. W., Shull, J. M. & Seab, C. G. 1982, ApJ, 262, L35

Cameron, M. & Liseau, R. 1990, A & A, 240, 409

Cardelli, J. A., Clayton, G. C. & Mathis, J. S. 1988, ApJ, 329, L33

Clarke, J. T. & Moos, H. W. 1981, in The Universe at Ultraviolet Wavelengths, ed. R. D. Chapman, NASA CP No. 2171, p. 787

Crenshaw, D. M., Bruegman, O. W. & Norman, D. J. 1990, PASP, 102, 463

de Boer, K. S. & Meade, M. R. 1981, NASA IUE Newsletter, No. 15, 33

Dopita, M. A. Binette, L. & Schwartz, R. D. 1982, ApJ, 261, 183

Edwards, S., Ray, T. & Mundt, R. 1991, in Protostars and Planets III, eds. E. Levy and J. Lunine (Tucson, Univ. of Arizona Press), in press

Goodrich, R. W. 1986, AJ, 92, 885

Herbig, G. H. 1974, Lick Obs. Bull., No. 658

Imhoff, C. L. & Appenzeller, I. 1987, in Exploring the Universe with the IUE Satellite, ed. Y. Kondo (Dordrecht: Reidel), p. 295

Lee, M. G., Böhm, K. H., Temple, S. D., Raga, A. C., Mateo, M. L., Brugel, E. W. & Mundt, R. 1988, AJ, 96, 1690

Miller, J. S. 1968, ApJ, 154, L57

Mundt, R. 1987, in Proc. IAU Symp. No. 122, Circumstellar Matter, ed. I. Appenzeller and C. Jordan (Dordrecht: Reidel), p. 147

Ortolani, S. & d'Odorico, S. 1980, A & A, 83, L8

Reipurth, B. 1991, in NATO Advanced Study Institute, "Physics of Star Formation and Early Stellar Evolution", in press

Schmidt, G. D. & Miller, J. S. 1979, ApJ, 234, L191

Schwartz, R. D. 1983a, ApJ, 268, L87

Schwartz, R. D. 1983b, Rev. Mex. Astr. Ap, 7, 27

Schwartz, R. D., Dopita, M. A. & Cohen, M. 1985, AJ, 90, 1820

Seaton, M. J. 1979, MNRAS, 187, 73p

Solf, J. 1987, A & A, 184, 322

Solf, J. & Böhm, K. H. 1987, AJ, 93, 1172

Solf, J., Böhm, K. H. & Raga, A. C. 1988, ApJ, 334, 229

Strom, K. M., Strom, S. E. & Kinman, T. D. 1974, ApJ, 191, L93

Turnrose, B. E. & Thompson, R. W. 1984, IUE Image Processing Information Manual, Computer Sciences Corporation

Figure Captions

Figure 1. Isophotic contour map of HH 24A based on a CCD image in the 6200-7000 Å band as presented by Solf (1987). Here we use this diagram to indicate approximately the region which is covered by the large aperture of IUE in our observations SWP 38033 and SWP 38102. (See text.)

Figure 2. The observed merged spectrum SWP 38102 (broken line) and the average of the merged spectra SWP 21518 and SWP 38102 (solid line) of HH 24A. Note the surprisingly good agreement between the two curves (see text). The spectra shown are not corrected for reddening and for the presence of the artifact spectrum. In this figure and in the diagrams in the following Figures 3, 4 and 5, the observed fluxes have been smoothed over 30 Å intervals (using a running mean).

Figure 3. The average of the observed spectra SWP 21518 and SWP 38102 (thin solid line), the reference artifact spectrum (broken line, see Crenshaw *et al.* 1990, their Figure 7) and the average spectrum corrected for the artifact spectrum (thick solid line) but not corrected for reddening.

Figure 4. Analogous to Figure 3, except that the average has been taken over the three spectra SWP 21518, SWP 38033 and SWP 38102.

Figure 5. The reddening corrected spectrum based on the average of SWP 21518, SWP 38033 and SWP 38102. Solid curves are based on the de-reddening using the Seaton curve (R=3.1 curve of Cardelli *et al.* 1988), broken curves are based on the use of the θ Orionis curve (R=5.4 curve of Cardelli *et al.* 1988).

Figure 6. A comparison of the observed flux distribution based on a de-reddening using the θ Orionis curve with the arbitrarily scaled relative distribution of the two photon continuum. The observed energy distribution has been smoothed (using a running mean) over 60 Å intervals.

Figure 7. The spatial distribution of the total intensity in the wavelength interval 1600

Å $\lesssim \lambda \lesssim$ 1800 Å. Open squares are based on the line-by-line spectra of SWP 38033, filled squares refer to SWP 38102. As spatial coordinate we have used the line number (see *e.g.*, Turnrose & Thompson 1984). A difference of 1 in the line number corresponds to 1."05 (arcseconds).

Figure 8. Comparison of the observed spatial distribution (filled squares) of the UV continuum in the 1600-1800 Å range (based on averaging over SWP 38033 and SWP 38102) to the observed [S II] 6716/6731 distribution (dash-dotted line, see text) and to the [S II] distribution (solid line) convolved with the IUE point-spread function. For comparison we also show the IUE point-spread function (broken line).

Table 1
IUE - (SWP) - Spectra of HH 24A

Image Nr.	Date	Exposure time (minutes)	Aperture Orientation Angle
SWP 38033	1990, Jan. 16	680	307°
SWP 38102	1990, Jan. 31	585	320°
SWP 21518	1983, Nov. 10	560	170°

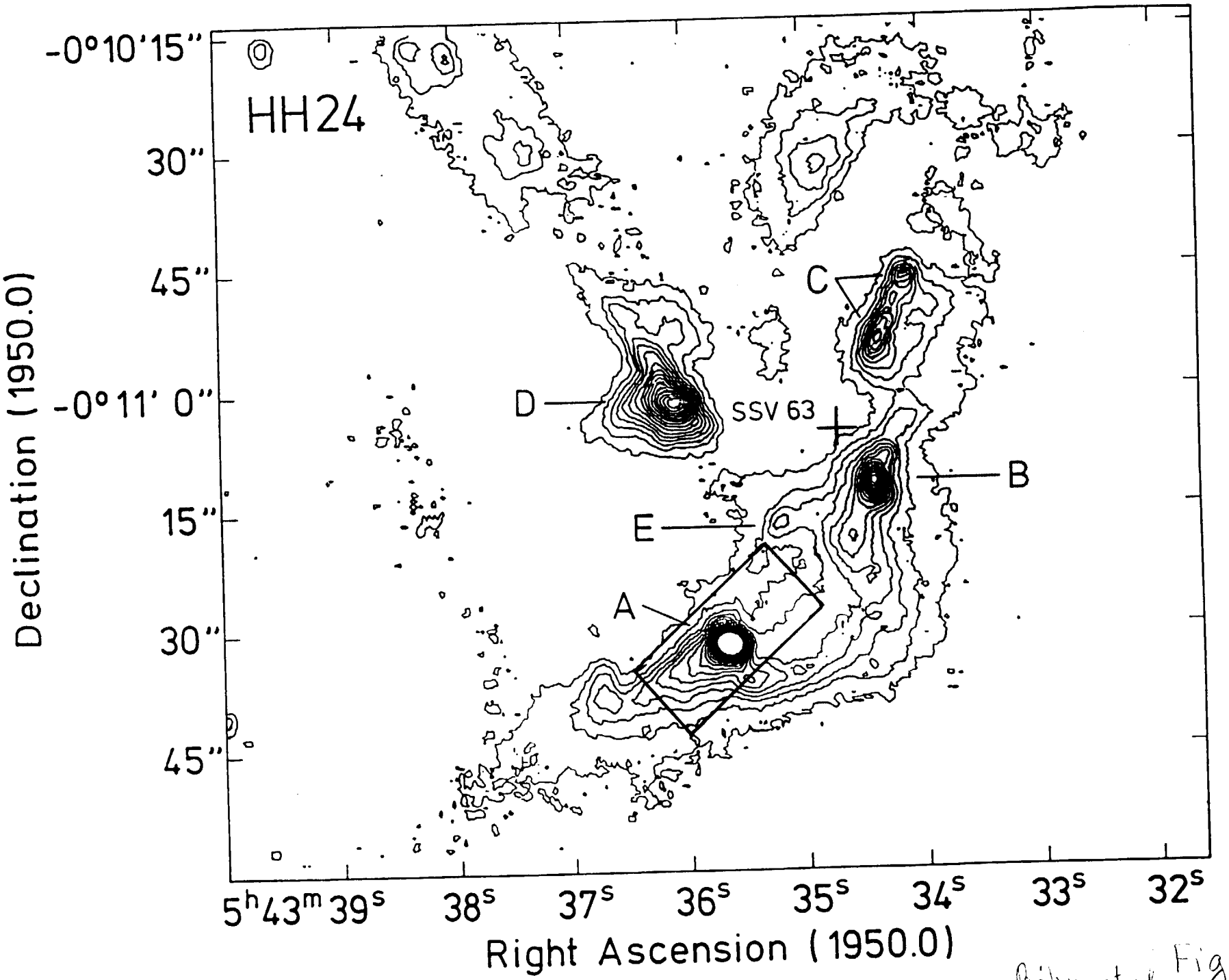

Bihm et al. Fig. 1

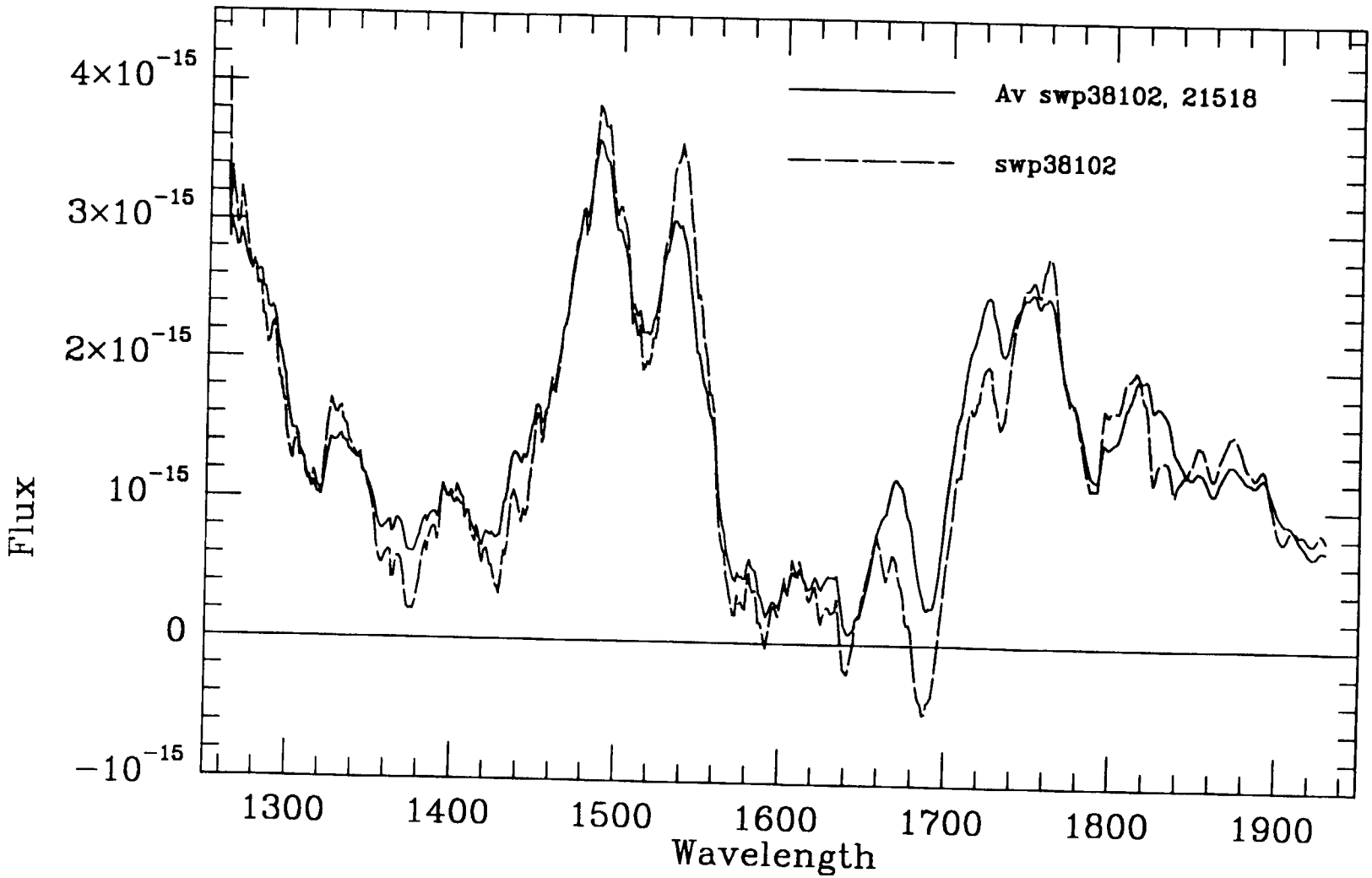

Böhm et al. Fig. 2

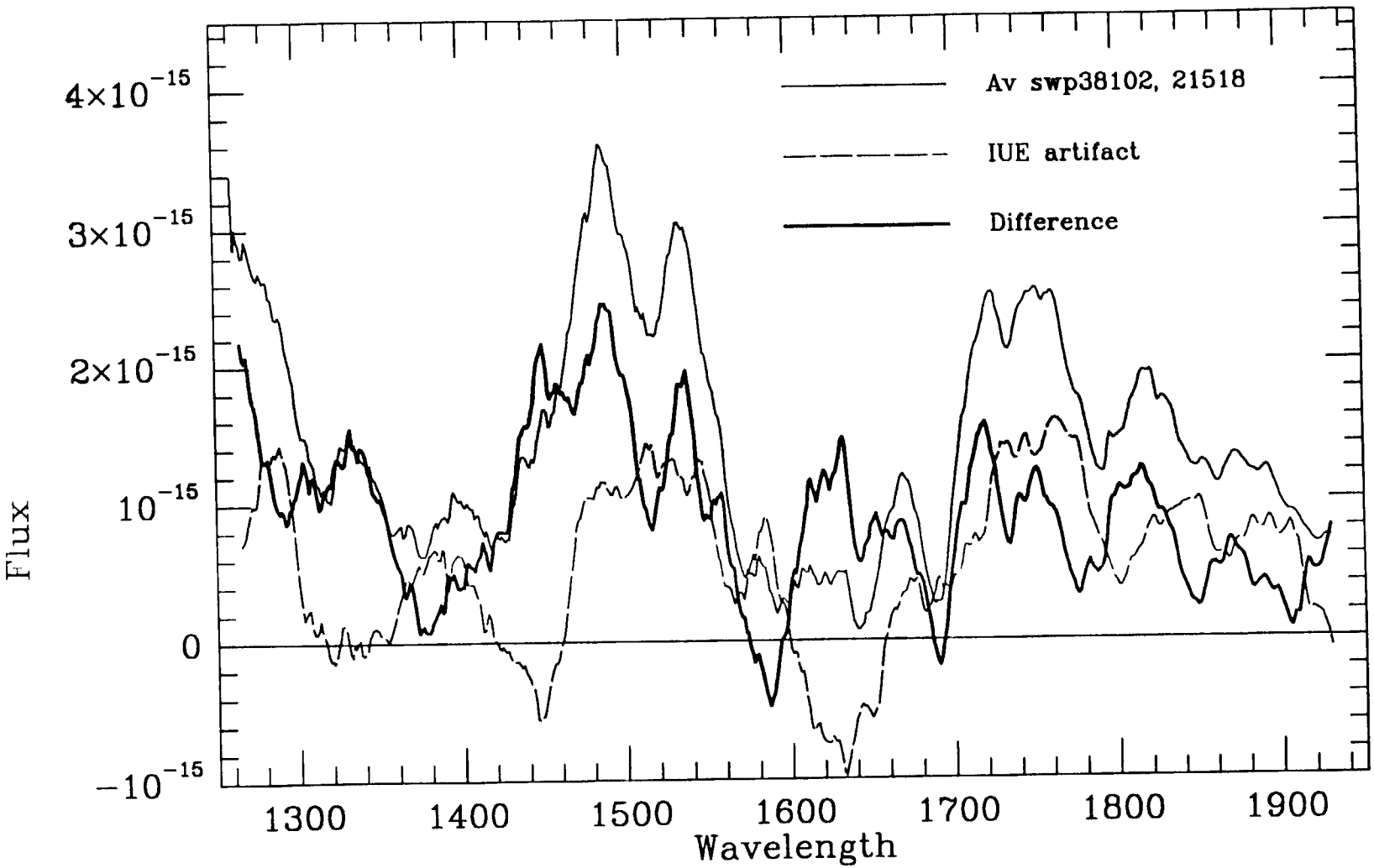

Böhm et al. Fig. 3

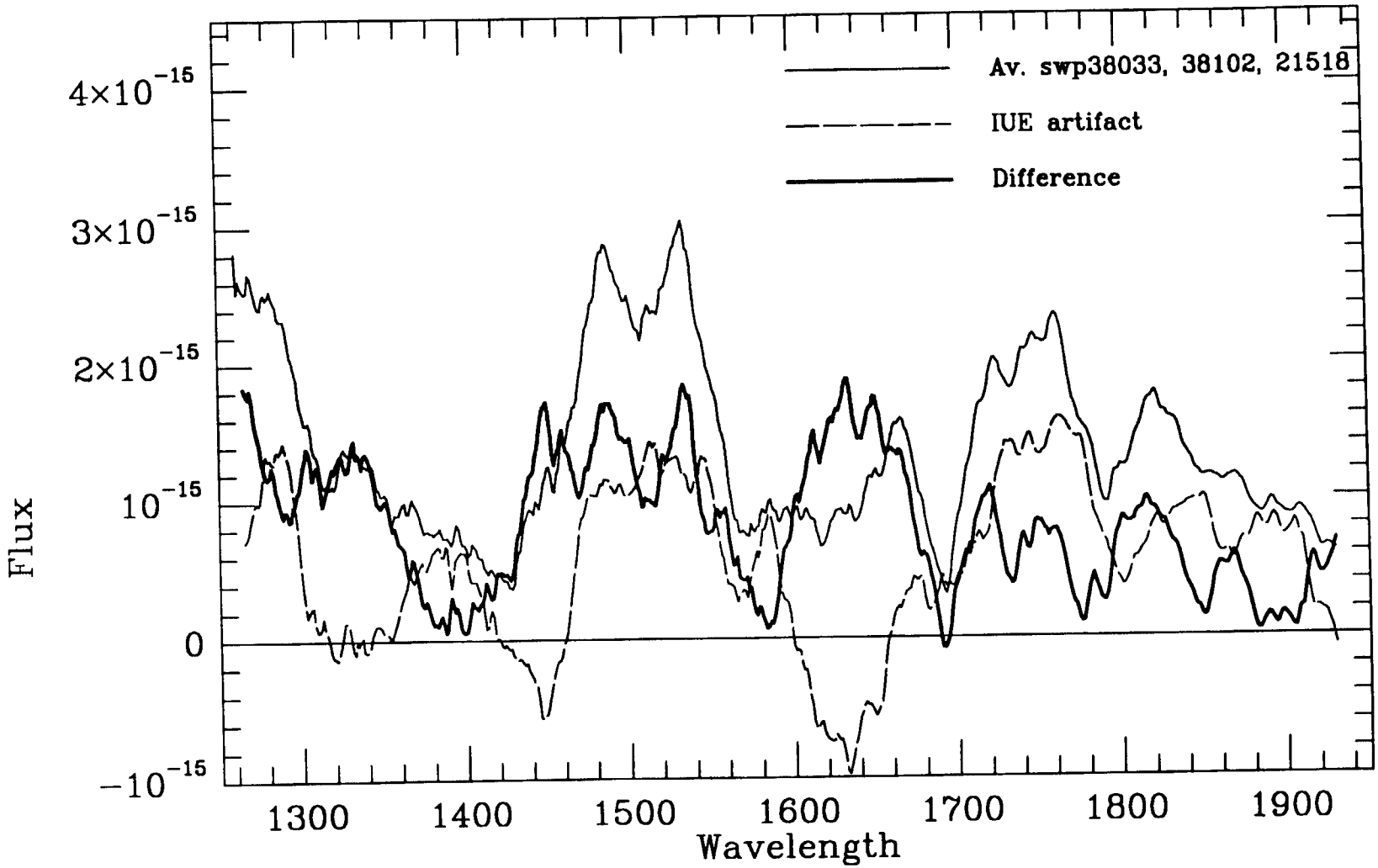

Bohlin et al., Fig. 4

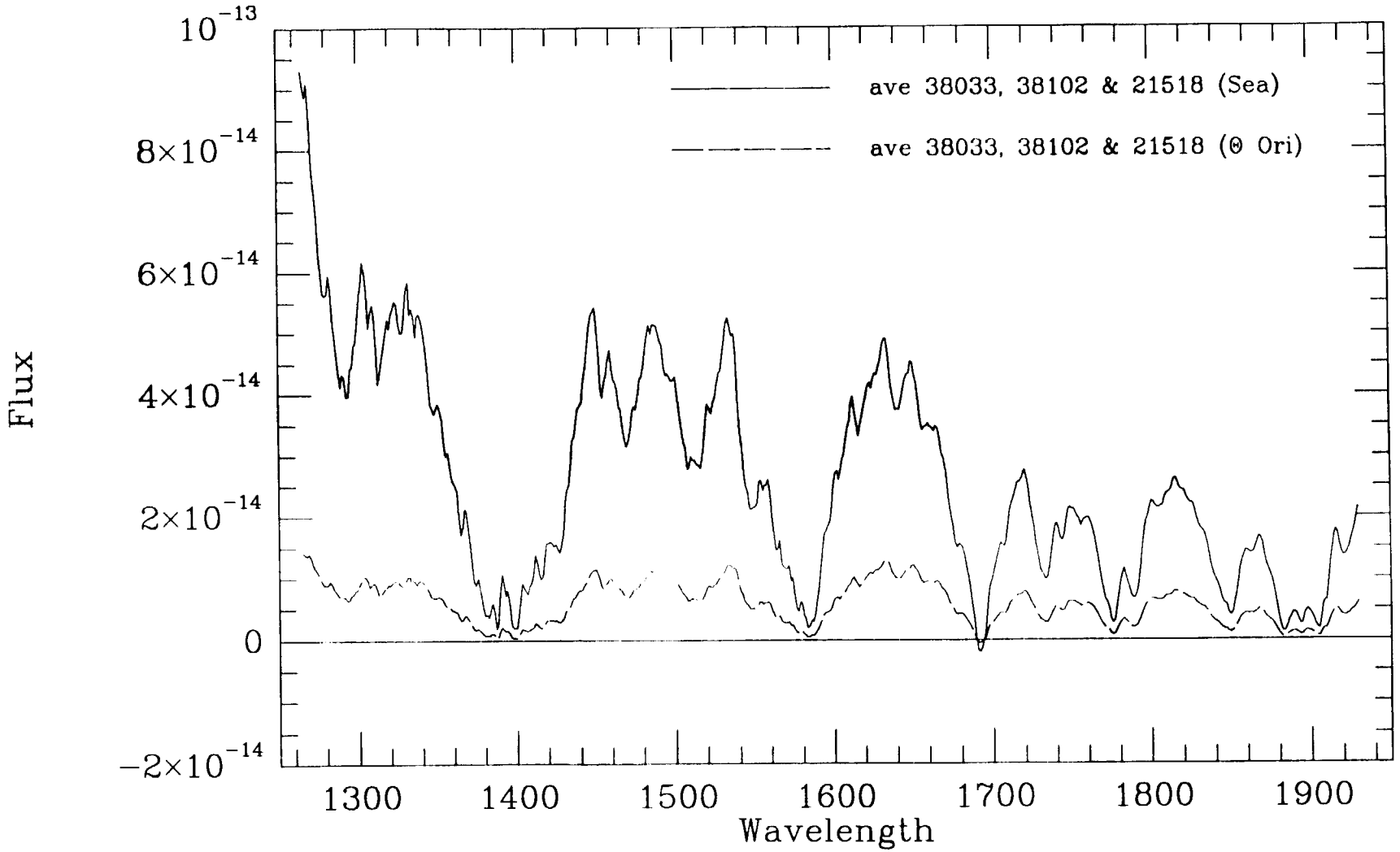

Böhm et al, Fig. 5

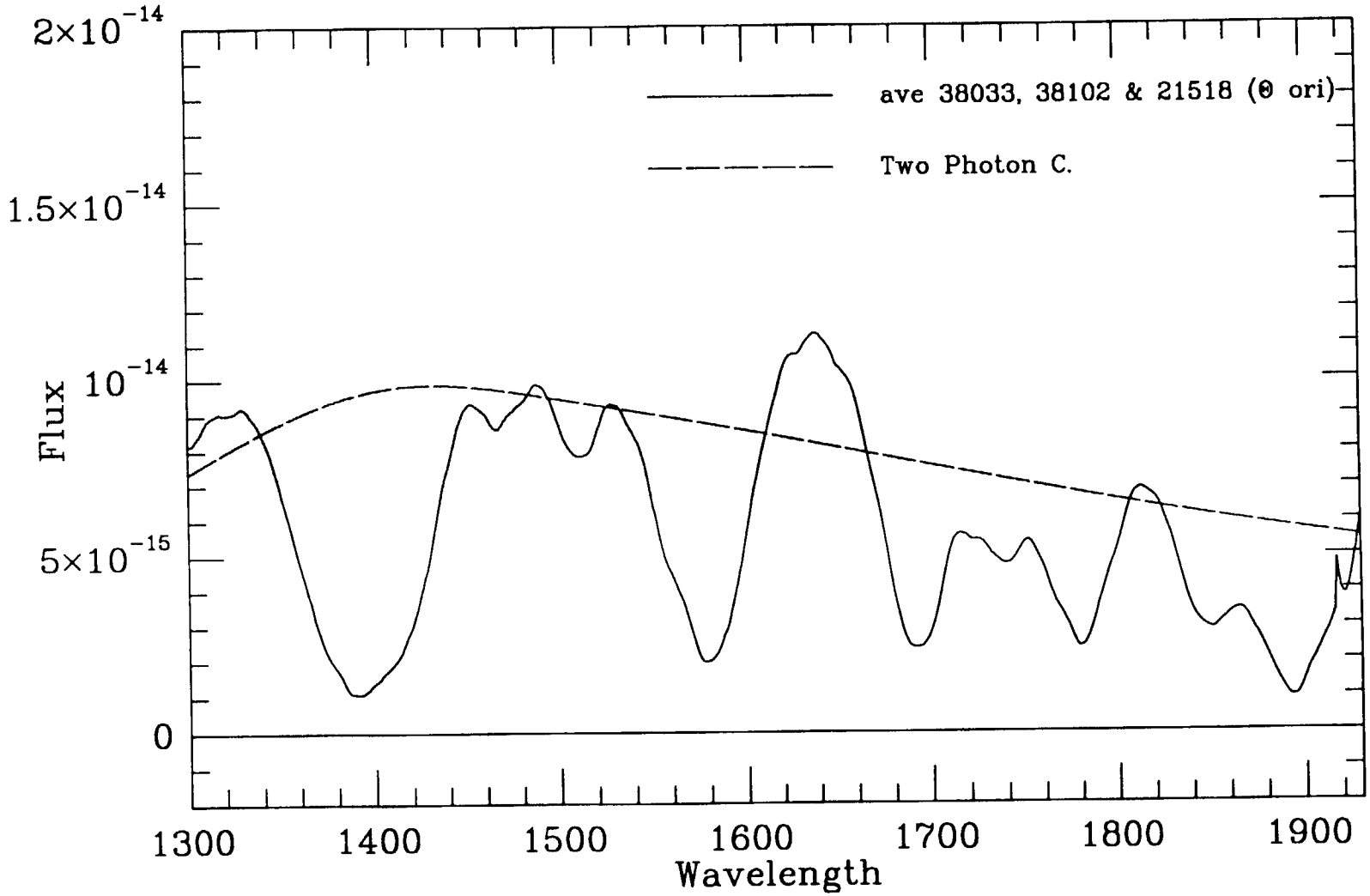

Böhm et al., Fig. 6

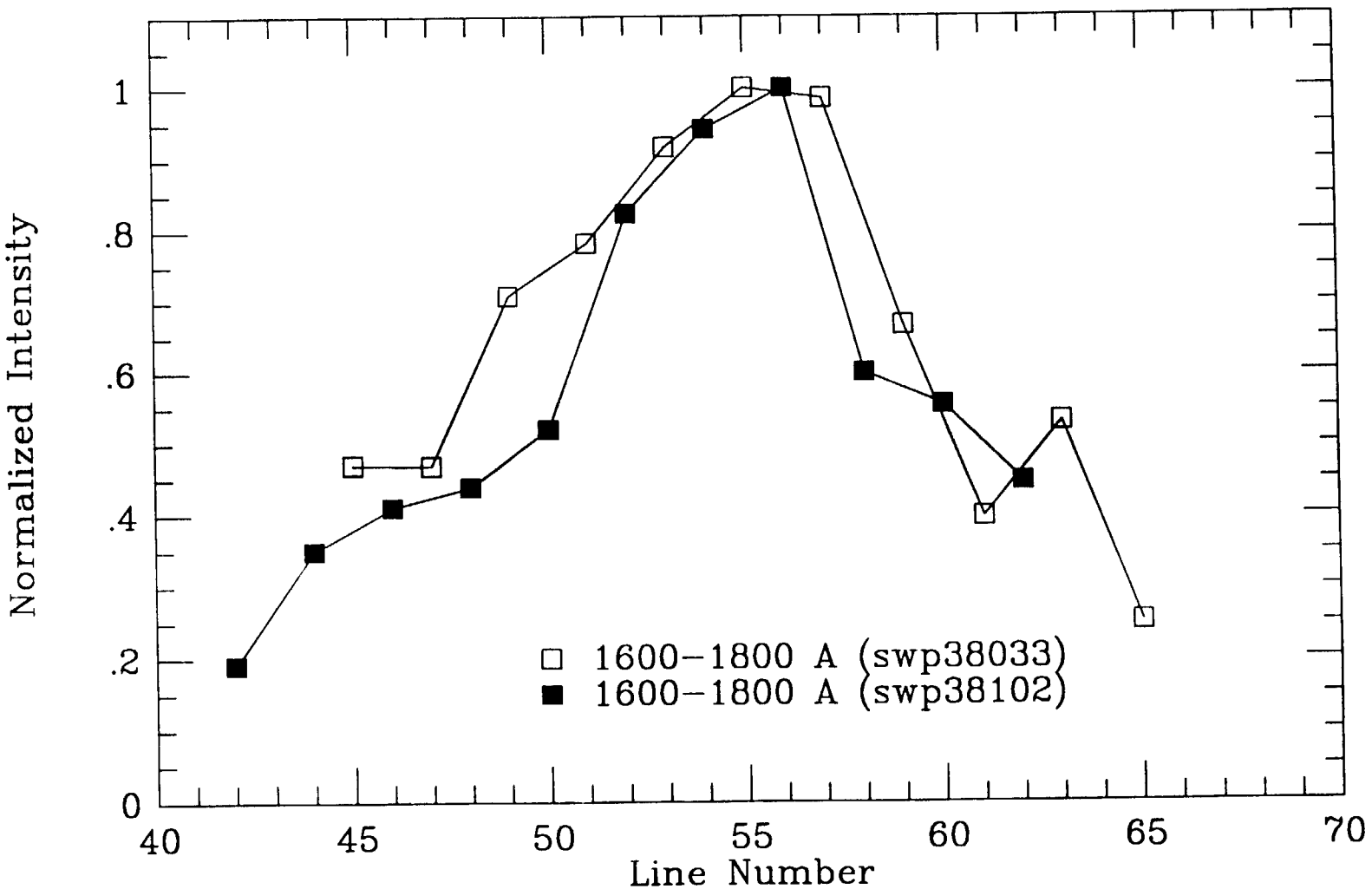

Sölln et al, Fig. 7

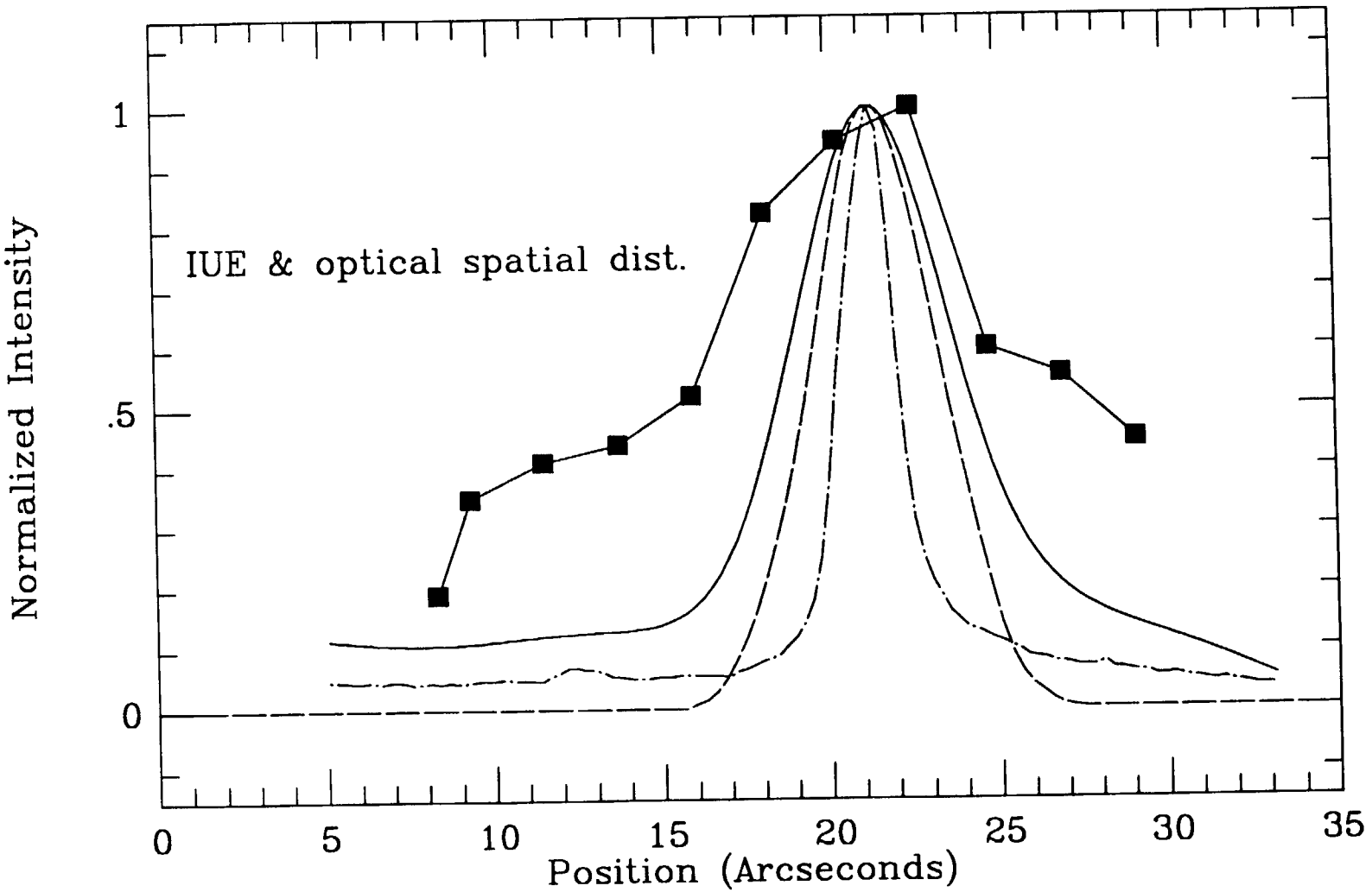

Böhm et al., Fig. 8